Journal of Magnetic Resonance **154,** 154–156 (2002)
doi:10.1006/jmre.2001.2465, available online at http://www.idealibrary.com on IDEAL®

COMMUNICATIONS

Scaling Laws in NMR Scattering via Dipolar Fields

S. M. Brown,* P. N. Sen,*,†,[1] and D. G. Cory*

*Department of Nuclear Engineering, Massachusetts Institute of Technology, Cambridge, Massachusetts 02139; and †Schlumberger-Doll Research, Ridgefield, Connecticut 06877

Received October 10, 2001

Breaking translational symmetry in magnetostatics imparts a scale dependence that is commonly investigated in physics (W. Warren *et al.*, 1993, *Science* 262, 2005–2008). An interesting and important example arises in nuclear magnetic resonance studies involving the dipolar mean field of adjacent nuclear spins where the scattering (transfer of spatial spin gratings) via intermolecular macroscopic fields carries a signature of the local spatial distribution of the spin density. For arbitrary geometry, the inverse problem of extracting this spin distribution from experiments is intractable. Here we point out a simple, universal crossover in the scaling behavior at the sample's characteristic length scale, ξ, of the species fluctuations in the sample along the measurement direction. This behavior is observed experimentally in an oil–water emulsion, an important representation of complex, heterogeneous, soft matter.

In statistical physics the inverse problem of extracting microscopic correlation lengths and times from the observed macroscopic response is, in general, intractable. Simple scaling relations, such as the Ornstein–Zernike (*2*) relation, are of supreme importance, since they easily yield the underlying correlation lengths. Analogously, in the time domain, macroscopic relaxation rates often depend on the product $\omega\tau$ of the *microscopic* correlation time τ and the probe frequency ω. For example, the pioneering work of Blombergen *et al.* (*3*) extracted the *microscopic* correlation time τ of water by noting the frequency ω_c where the *macroscopic* relaxation rate changes rapidly as a function of the probing (Larmor) frequency.

The scattering or transfer of transverse spin magnetization in NMR experiments described here is carried by the magnetostatics dipolar mean field of one phase seen by the other. Remarkably, standard magnetostatics (*4*) is scale independent, and, as such, contains no information of the absolute size. When the translational symmetry is broken, such as by imparting on the system a spatially dependent magnetization, the well-known incipient logarithmic divergence is removed, and new interesting results emerge (*5*). With a new scale available from that of the impressed symmetry-breaking field (SBF), it is possible to probe system length scales. The SBF becomes localized near the interface, and is quite analogous to a skin-depth phenomenon for a time-varying electromagnetic field in a dissipative medium (however, here we are concerned with the DC field). This localization near the interface provides a measure of the features near the interface. The localized nature of the field induced by a sinusoidal modulation of magnetic polarization was realized by Warren *et al.* (*1*), and the concept has subsequently been demonstrated by Warren and co-workers (*6*) and by Bowtell and co-workers (*7–9*). Here we recast their experiment and analysis to emphasize a break in the scaling of the NMR response versus wavenumber. The recognition of this scaling law permits a simple and model-independent extraction of the characteristic length scale of the sample.

The scaling behavior can be developed in direct analogy to indirect scattering. Recently, it has become well appreciated (*10–12*) that an experiment where the wave vector-dependent magnetization grating is encoded and subsequently decoded constitutes an NMR scattering experiment with the scattering amplitude given by an intermediate scattering function completely analogous to that in neutron scattering. So far, most NMR scattering experiments deal with self-scattering. The SBF experiments are unique in that they involve the transfer of the grating from one phase to another. These methods can extract the interphase Debye structure factors (*13*).

The physical origin of the scaling behavior induced by the SBF is explained by following the transfer of magnetization gratings between phases. Given an amplitude-modulated grating in the water spin magnetization $M_z^a \propto \cos(|\mathbf{q}|z)$, where $\mathbf{q}$ is the wave number $q = 2\pi/\lambda$, the second medium (oil) sees a spatially modulated local mean field. Following excitation, the oil spins precess at a rate dependent on this local field, and after some time, the water grating is written into the phase of the oil magnetization. The insets of Fig. 1 show the mean field inside included spheres of oil at different wavelengths of the surrounding water magnetization grating. There are clearly two distinct regimes. At long wavelengths, the field is relatively uniform

[1] To whom correspondence should be addressed. E-mail: sen@ridgefield.sdr.slb.com.

1090-7807/02 $35.00

inside the sphere, but the magnitude depends on $\mathbf{q}\cdot\boldsymbol{\xi}$, where ξ is the bubble radius for a spherical inclusion. At short wavelengths, the field is localized near the interface, decaying approximately exponentially with $\mathbf{q}\cdot\boldsymbol{\xi}$. This change in scaling laws can be developed rather simply, and then applied to obtain structural information at the interface.

At wavelengths that are long relative to the length scale of the inclusion, the field is well defined by an expansion including only low-order spherical harmonics. The lowest order harmonic that contributes to the field is the $l=1$ harmonic, and it dominates the field intensity at long λ. Here the field due to the $l=1$ harmonic does not vary with position inside the bubble, but its strength depends on the scaled variable $\mathbf{q}\cdot\boldsymbol{\xi}$. The higher harmonics are responsible for the field variation inside the bubble, but contribute little to the field intensity. The field due to the $l=1$ harmonic, for a spherical inclusion imbedded in an infinite medium, is given by

$$B_{\text{dipolar}} \approx -2M_{0,\text{water}}\mu_0 \frac{j_1(\mathbf{q}\cdot\boldsymbol{\xi})}{(\mathbf{q}\cdot\boldsymbol{\xi})}\cos(|\mathbf{q}|h), \qquad [1]$$

where j_1 is the first-order spherical Bessel function of the first kind, μ_0 is permeability of free space, and $|\mathbf{q}|h$ is the phase offset of the grating at the center of the bubble which is located at height h measured along the grating in the host medium. This form applies for $\mathbf{q}\cdot\boldsymbol{\xi}\leq 1$, but in practice, we find that it continues to hold beyond its expected range of validity (see Fig. 1). For arbitrary shape this result generalizes to a field that is uniform over the inclusion and whose strength goes as $B_{\text{dipolar}} \rightarrow C_1 + C_2(\mathbf{q}\cdot\boldsymbol{\xi})^2$, where the constants, C_1 and C_2, will depend on the shape of the inclusion.

For $\lambda \leq \xi$ the dominating aspect of the internal mean field is the transition from the average field effects described above to a more local effect, where the field falls off in the interior of the bubble. To determine the scaling law in this region, it suffices to consider the mean field outside an infinite half-space (i.e., a wall) of modulated longitudinal water magnetization along the z-direction. The mean field depends exponentially on the scaled distance, $q\rho$, asymptotically as

$$B_{\text{dipolar}} \approx \frac{\mu_0 M_{0,\text{water}}}{4} e^{-|\mathbf{q}|\rho}\cos(|\mathbf{q}|h), \qquad [2]$$

where ρ is the transverse distance from the interface. For arbitrary shapes, an approximate exponential dependence of the mean field on scaled distances from the interface will be observed for $\mathbf{q}\cdot\boldsymbol{\xi} > 1$. Numerical results for spherical inclusion are shown in Fig. 1. Clearly, the flat-wall approximation captures the correct asymptotic behavior.

The transition between short and long wavelength behavior of the field imparts the scaling behavior of the signal in the experiment described here. The specific system under study is a poly-disperse oil/water emulsion created by suspending oil bubbles in an aqueous gel. The average diameter, 2ξ, of the bubbles was determined visually using a microscope to be approximately 150 μm with sizes ranging from 25 to 320 μm. Of course in this heterogeneous sample there is a distribution of characteristic length scales and the roundness of the break in Fig. 1 reflects this. The experimental NMR pulse sequence is shown in Fig. 2. This pulse sequence is essentially that used by Bowtell and Robyr (*7*) to probe dipolar field behavior in simple cylindrical samples. The wave vector of the water modulation is $\mathbf{q} = \gamma g \tau s$, where γ is the gyromagnetic ratio, g is the strength of the applied gradient, τ is the time during which the gradient is applied, and s is the direction of the applied gradient. The experiment refocuses the resulting first spatial Fourier component in the oil, and the oil echo magnitude is recorded as a function of the wavelength, λ, of the applied modulation.

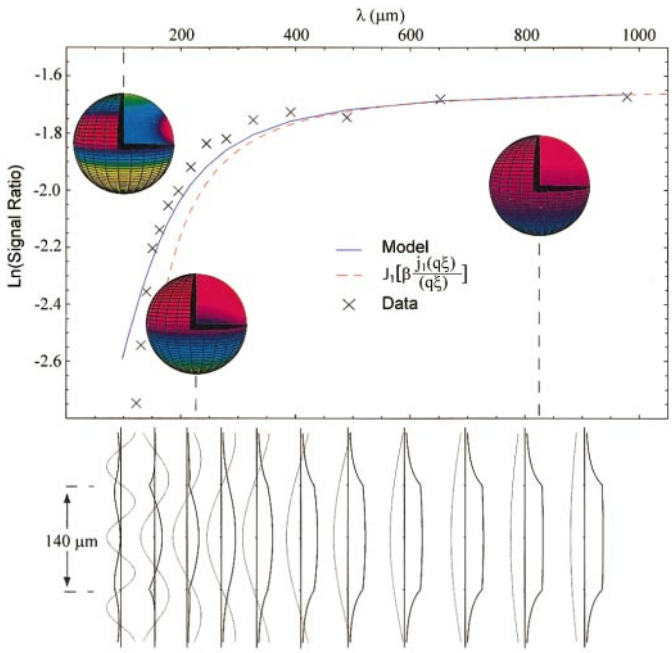

FIG. 1. NMR signal behavior versus applied wavelength. In NMR scattering via the dipolar field, a sharp change near $\mathbf{q}\cdot\boldsymbol{\xi}\approx 1$ is observed in the natural logarithm of the normalized NMR signal versus the wavelength λ of the applied magnetization grating. The blue line (solid) displays the results of a numerical calculation including spherical harmonics up to order 11 for the scattering from a continuous medium to imbedded spheres. The crosses are the experimental data points. The red line (dashed) shows the behavior of the $l=1$ harmonic with $\beta = 2\eta M_{0,\text{water}}\gamma\mu_0 t$, where η is a constant attenuation factor that fits the model curve to the two rightmost points of the experimental data (see discussion in text). The insets show the calculated field intensity inside the oil bubbles at the indicated wavelengths. The north and south poles of the sphere lie on the z-axis. Red (+) and orange (−) show the highest intensities and light blue indicates zero intensity. Note how the field behavior changes from a global behavior at long wavelengths, to a localized interfacial interaction at short wavelengths. The series of plots below shows the z-component of the magnetic flux density along the longitudinal axis of the bubbles. The water magnetization gratings (magnitude not to scale) are shown for comparison as the light gray curves that overlay the darker flux density curves. Note that the flux density along the center of the bubbles decreases in intensity as the wavelength approaches the length scale of the system. In the short wavelength region, the signal magnitude is controlled by exponential behavior in the equatorial regions of the bubble.

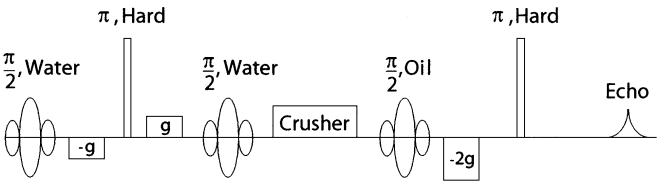

FIG. 2. Experimental NMR pulse sequence. The NMR pulse sequence used to extract structural information in the emulsion experiment. The first $\pi/2$-pulse selectively tips the water magnetization into the transverse plane. The two gradients of opposite polarity write a grating in the water spin magnetization. The crusher gradient in the center of the sequence removes all transverse water magnetization, leaving only z-directed modulated water magnetization. The hard π-pulses refocus field inhomogeneities, largely caused by susceptibility fields. The final gradient pulse $-2g$ selects the first spatial Fourier component of the oil magnetization induced by the presence of the water's dipolar field. The gradient strength, g, is varied to map out the data in Fig. 1.

The water mean field as seen by the oil spins imparts a phase grating to the transverse oil magnetization. This oil magnetization grating consists of harmonics of the original water grating, from which the first Fourier component is selected by a gradient echo. Figure 1 displays the natural logarithm of the intensity of the fundamental Fourier component of the oil grating as a function of the wavelength of the applied modulation. The signal shows a strong crossover in scaling at $\mathbf{q} \cdot \boldsymbol{\xi} \approx 1$.

In the long wavelength region, the signal is described by

$$\text{Normalized Signal} = J_1\left[\frac{2\eta M_{0,\text{water}}\gamma\mu_0 t j_1(\mathbf{q}\cdot\boldsymbol{\xi})}{(\mathbf{q}\cdot\boldsymbol{\xi})}\right], \quad [3]$$

where J_1 is the first-order Bessel function of the first kind. At long wavelengths, the signal approaches a constant value that is independent of the system's length scale. η is the volume fraction of water that contributes to the grating. This is reduced from the water volume fraction by the diffusive attenuation of water in the susceptibility field of the bubble. Here, the actual volume fraction of water (0.76) is reduced to $\eta = 0.49$ at a time of 80 ms.

In the short wavelength limit, the signal decreases dramatically,

$$\text{Normalized Signal} \approx \frac{\gamma\mu_0 M_{0,\text{water}} t}{8|\mathbf{q}|\cdot\boldsymbol{\xi}}, \quad [4]$$

since the signal is restricted to spins near the surface, and is proportional to

$$\frac{\text{Surface Area} \times \lambda}{\text{Volume}} \propto \frac{1}{\mathbf{q}\cdot\boldsymbol{\xi}}.$$

In summary, we have described a simple change in scaling laws appropriate for NMR scattering involving dipolar fields. The characteristic length scale can thus be extracted in a simple and robust manner. Based on universality of this change in scaling, it is now possible to employ NMR scattering via dipolar fields to measure the characteristic length scales of heterogeneous samples.

ACKNOWLEDGMENTS

This work was partially funded by the National Institutes of Health (NIH). S. M. Brown was funded by the U.S. Navy's Civilian Institutions Program (CIVINS).

REFERENCES

1. W. Warren, W. Richter, A. Andreotti, and B. Farmer, Generation of impossible cross peaks between bulk water and biomolecules in solution NMR, *Science* **262,** 2005–2008 (1993).
2. I. Ornstein and F. Zernike, *Proc. Acad. Sci.* (*Amsterdam*) **17,** 793 (1914).
3. N. Blombergen, E. M. Purcell, and R. V. Pound, Relaxation effects in nuclear magnetic resonance absorption, *Phys. Rev.* **73,** 679–712 (1948).
4. See, for example, J. C. Maxwell, "Electricity and Magnetism," 1st ed., Clarendon Press, Oxford (1873), or Lord Rayleigh, *Philos. Mag.* **34,** 481 (1892).
5. G. Deville, M. Bernier, and J. Delrieux, NMR multiple echoes observed in solid He-3, *Phys. Rev. B* **19,** 5666–5688 (1979).
6. W. Richter, W. Warren, and Q. He, Imaging with intermolecular multiple quantum coherences in solution nuclear magnetic resonance, *Science* **267,** 654–657 (1995).
7. R. Bowtell and P. Robyr, Structural investigations with the dipolar demagnetizing field in solution NMR, *Phys. Rev. Lett.* **76,** 4971–4974 (1996).
8. P. Robyr and R. Bowtell, Nuclear magnetic resonance microscopy in liquids using the dipolar field, *J. Chem. Phys.* **106,** 467–476 (1997).
9. P. Robyr and R. Bowtell, Measuring Patterson functions of inhomogeneous liquids using the nuclear dipolar field, *J. Chem. Phys.* **107,** 702–706 (1997).
10. R. M. Cotts, *Nature* **351,** 443 (1991).
11. P. T. Callaghan, A. Coy, D. MacGowan, K. J. Packer, and F. O. Zelaya, *Nature* **51,** 467 (1991).
12. D. G. Cory and A. N. Garroway, *Magn. Reson. Med.* **14,** 435 (1990).
13. P. Debye, H. R. Anderson, and H. Brumberger, *J. Appl. Phys.* **28,** 679 (1957).